JOURNAL OF ZOOLOGICAL SYSTEMATICS AND EVOLUTIONARY RESEARCH

Accepted on 17 March 2013
J Zoolog Syst Evol Res doi: 10.1111/jzs.12020

[1]*Faculty of Natural Resources and Environment, Ferdowsi University of Mashhad, Mashhad, Iran;* [2]*Ghent University, Evolutionary Morphology of Vertebrates, Gent, Belgium*

Cranial variation in *Meriones tristrami* (Rodentia: Muridae: Gerbillinae) and its morphological comparison with *Meriones persicus*, *Meriones vinogradovi* and *Meriones libycus*: a geometric morphometric study

Fatemeh Tabatabaei Yazdi[1] and Dominique Adriaens[2]

Abstract

Jirds (genus *Meriones*) comprise a group of rodents, of which the biodiversity is still poorly known. Reason for this is that several species of similar morphologies are known to occur sympatrically. In the north-west of Iran, four such species occur: *Meriones tristrami, Meriones persicus*, *Meriones vinogradovi* and *Meriones libycus*, prone to several issues of taxonomical ambiguity. A proper characterization of morphological distinctiveness between these species, in relation to the variation within species, could provide the required information for species diagnosis and identification. As some cranial characters of *M. tristrami, M. persicus* and *M. vinogradovi* are quite similar, demarcations of species-specific phenotypic variation have proven to be difficult. To tackle this problem, this study involves a geometric morphometric analysis of skull shape and size, incorporating a large representative sample of these four species, originating from most parts of their natural distribution range (especially for *M. tristrami*). It is first tested whether *M. tristrami* can be distinguished from the other sympatric species, and if so, to what degree the species shows a geoclimatic pattern in its skull shape and size when comparing different populations. The shape and size analyses show that *M. libycus* can be distinguished because of its largest skull and the relatively largest tympanic bulla, and that *M. tristrami* can be distinguished from the other species. At an intraspecific level in *M. tristrami*, the Iranian groups (Qazvin and west Iran) do not differ in shape among them, but do so in skull size. They could, however, be distinguished in skull shape from the non-Iranian populations included (Turkey and Jordan). To what degree this continuous data can now be translated into discrete and diagnostic features, useful for taxonomic purposes, remains to be studied.

Key words: Jird – morphological variation – Muridae – Rodentia – skull

Introduction

Tristram's jird (*Meriones tristrami* Thomas, 1892), a polytypic rodent species (Yiğit and Çolak 1998), is one of the *Meriones* species occurring sympatrically in the north-west of Iran, together with *Meriones persicus*, *Meriones vinogradovi* and *Meriones libycus*. *Meriones tristrami* is distributed from Israel, Lebanon, and western Jordan to Turkey, Syria, northern Iraq, north-west Iran (Azerbaijan, Qazvin, Kordestan and ranging eastwards up to Tehran and southwards up to Hamedan) and Transcaucasia (Fig. 1, dashed line). *Meriones persicus* Blanford, 1875 is distributed along Iran, Iraq, Transcaucasia, Turkey (east Anatolia), Turkmenistan, Afghanistan and Pakistan (west of the Indus River). *Meriones vinogradovi* Heptner, 1931 is distributed along northern Iran, Turkey (east of Anatolia), northern Syria, Armenia and Azerbaijan. *Meriones libycus* Lichtenstein, 1823 is distributed from North Africa through Saudi Arabia, Jordan, Iraq, Syria, Iran, Afghanistan and east through Turkmenistan, Uzbekistan and south Kazakhstan to western China (for a more detailed map, see Darvish 2011) (Misonne 1959; Lay 1967; Musser and Carleton 2005; Karami et al. 2008). Although these rodents have been given a species status based on their external and cranial characters (e.g. fur colour, tail length and bulla inflation), intraspecific variation resulting in overlapping ranges in their cranial diagnostic features resulted in an ambiguous classification and debated taxonomy (Harrison 1972; Chevret and Dobigny 2005; Naseri et al. 2006). Only *M. libycus* can be clearly distinguished from the other species by its cranial traits, such as the existence of an inflated tympanic bulla (anterior lip of external auditory meatus conspicuously swollen up to the level of the zygomatic process of the temporal bone), the mastoid portion extending beyond the occiput and a suprameatal triangle being virtually closed posteriorly. In *M. tristrami, M. persicus* and *M. vinogradovi,* the tympanic bulla is less swollen, the suprameatal triangle is small and closed posteriorly and the anterior rim of auditory meatus does not come into contact with the posterior root of the zygomatic arch (Darvish 2011).

Because of a small morphological difference (a white spot covering the area around the eyes in *M. tristrami*, but being supraorbital only in *M. persicus*) (Benazzou 1984; Yiğit and Çolak 1999), *M. tristrami* was identified as a sibling species with *M. persicus* (Yiğit 1999). Also *M. vinogradovi* has been considered a sibling species to *M. tristrami*, because of a very similar cranial and dental morphology (Harrison 1972).

Although many studies on various aspects of the biology of *M. tristrami*, like geographical distribution, morphology, and karyology, have been conducted, their focus has been regional and only concerning Turkish populations (Misonne 1957; Yiğit et al. 1995; Yiğit et al. 1998, 1999, 2006; Coşkun 1999; Demirbaş and Pamukoğlu 2008). Only a few studies have been carried out on the karyology, geographical distribution and morphology of Iranian Tristram's jird (e.g. Misonne 1959; Lay 1967; Yiğit et al. 2006). They already briefly revealed karyological and morphological differences between some Iranian and Turkish *M. tristrami* populations, suggesting the potential existence of numerous subspecies. For example, six Turkish subspecies of *M. tristrami* were described based on morphology (mostly external characters) and karyology (Demirbaş and Pamukoğlu 2008). As such, the existence of similar levels of intraspecific variation in populations from the north-west of Iran may be expected to exist, where geographical heterogeneity (hence niche heterogeneity) is even more elaborate. Misonne (1959) has already shown shape differences that exist between *M. tristrami* populations from Iran and those from Turkey (the region of Urfa-Akcakale in southern Turkey), and even suggested that they belong to distinct morphological groups. Also, the distribution of this species in Iran is apparently disrupted, with populations occurring in

Corresponding author: Fatemeh Tabatabaei Yazdi (f.tabatabaei@um.ac.ir; fatemeh.tabata@gmail.com)
Contributing author: Dominique Adriaens (dominique.adriaens@ugent.be)

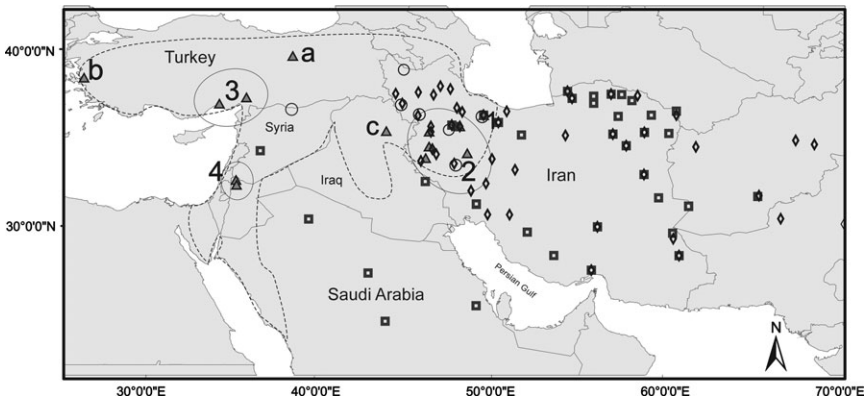

Fig. 1. Map showing the sampling localities of the *Meriones* species: ▲ *Meriones tristrami,* ◆ *Meriones persicus*, ■ *Meriones libycus* and ○ *Meriones vinogradovi*. Ovals show grouped *M. tristrami* sampling localities that were considered in this study. Localities indicated by a, b and c represent single specimens (other localities are represented by multiple specimens and were grouped because of geoclimatical closeness). The dashed line indicates the total distribution range of *M. tristrami*

the hill slopes of Alborz Mountains range and in the Zagros Mountains (Karami et al. 2008). However, these regional studies that have already been carried out are insufficient to clarify the taxonomical, morphological and phylogenetic relationships in these rodents (Misonne 1959; Lay 1967; Yiğit et al. 2006).

The distribution of *M. tristrami* is reported to be limited to areas with more than 100 mm rainfall annually, although there are some exceptions including the north-east of Jordan and the eastern Syrian Desert. This species occurs in the Irano-Anatolian region, considered a biodiversity hotspot by Conservation International. It also includes highlands of the central and eastern Anatolian Plateau, as well as the Zagros and Alborz Mountain ranges (http://www.conservation.org).

Since taxonomical clarifications and the recognition of natural groups are important for the understanding of biodiversity, a more elaborate quantification of morphological variation along a wide distribution range of these sympatrically occurring *Meriones* species is needed. Especially *M. tristrami* forms an interesting case, considering its shared distribution with three other *Meriones* species and its taxonomic ambiguity. Clarifying the taxonomical issues is essential for a better understanding of the poorly known biodiversity in the Iranian region, in particular of *Meriones*. As such, this study first aimed to test whether *M. tristrami* can be distinguished from its sympatric congeners based on cranial shape and size. As the results obtained supported this hypothesis, we further explored the pattern of intraspecific variation within that species, to test whether the geographical spreading of Iranian versus other populations is reflected in cranial shape and size variation too. Finally, the results on cranial shape and size patterns (both inter- and intraspecific) are discussed in relation to how they could be used to construct usable identification keys.

Materials and Methods

Specimens collection

Skulls were obtained from the collections of the Smithsonian Natural Museum of Natural History (Washington, DC, USA), the Field Museum of Natural History (Chicago, IL, USA), the Natural History museum (London, UK), the Muséum National d'Histoire Naturelle (Paris, France), the Natural History Museum of Ferdowsi University (Mashhad, Iran) and the Royal Belgian Institute of Natural Sciences (Brussels, Belgium). A list of examined specimens with catalogue number is available in the Appendix 1.

A total of 536 intact skulls belonging to *M. tristrami* ($n = 53$), *M. persicus* ($n = 221$), *M. libycus* ($n = 220$) and *M. vinogradovi* ($n = 42$) were used. Specimens were identified based upon the external (e.g. tail morphology) and cranial criteria, including several features related to the auditory bulla (e.g. suprameatal triangle and point up to which the auditory bulla reaches) using published identification keys (Chaworth-Musters and Ellerman 1947; Osborne and Helmy 1980). Information on collection labels was used as additional information for the identification. So far, sexual dimorphism has never been observed in these taxa, both at the level of skull size and shape (Darvish 2009). As such, specimens of both sexes were pooled for further analyses. Juvenile specimens, identified based on the eruption and amount of wear on the molar (Petter 1959; Tong 1989; Yiğit 1999; Pavlinov 2008), were excluded to avoid shape variation due to ontogenetic allometries. The origin of these skulls represents a wide range of the natural distribution of these species (Fig. 1).

For the analysis of intraspecific variation in *M. tristrami*, specimens were plotted on a map according to the geographical coordinates of the sample location, using ArcGIS, ArcMap 9.2 (Fig. 1). In Table 1, sampling localities and sample grouping are given. For the analysis on interspecific variation, similar information for the other studied species is provided in Appendix 2.

To avoid that sample sizes per group to be compared would be too low with respect to the number of variables in the canonical variate analysis (CVA) (Kovarovic et al. 2011), samples of *M. tristrami* were pooled according to their geoclimatical proximity into four larger operational groups (Jordan, Turkey, Qazvin and west Iran). With the absence of direct evidence of population boundaries (such as population genetic substructures), geoclimatical affinities are used as proxies. Geoclimatically isolated samples, or samples having only one specimen, were not included in the analysis. Excluded specimens are those of *M. t. lycaon* (Thomas, 1919) and *M. t. blackleri* (Thomas, 1903). These specimens were two type specimens that have been synonymized with *M. tristrami* by Musser and Carleton (2005), and which were studied here in order to assign specimens to a species.

Geometrical morphometrics and data collection

Several studies suggest that geometric morphometrics is statistically powerful and visually effective (Bookstein 1991; Rohlf and Marcus 1993; Adams et al. 2004; Cardini and Elton 2009). The use of landmark data to quantify variation in both skull size and shape in mammals is sufficiently powerful to resolve issue where even subtle variation is at hand (Rohlf and Marcus 1993; Fadda and Corti 2000; Barciova and Macholán 2006; Cardini et al. 2007; Macholàn et al. 2008; Cardini and Elton 2009). As such, we applied this approach for a taxonomical assessment of *M. tristrami*.

Landmark data were obtained from photographs taken with a Nikon D70 digital reflex camera (Nikon Corp., Tokyo, Japan) using a Sigma 105 mm macro lens (Sigma Corp., Ronkonkoma, NY, USA) at 5 megapixels using a standardized protocol. The camera was placed on a tripod parallel to the ground plane. To allow a standardized positioning of the cleaned skulls (only intact skulls being used), they were mounted in a box with glass pearls. Left–right symmetry on the ventral and dorsal

Table 1. Overview of the sampling localities of *Meriones tristrami* used in this study. Specimens from type localities included are those of *Meriones blacklery lycaon* (*M. t. lycaon*) (*a*) and *Meriones tristrami* (*M. t. blackleri*) (*b*). Also, a single specimen of Kirkuk was included that was not pooled with the other locations (*c*)

Country	Province	Location	Lat.	Lon.	Sample size	Group
Iran	Qazvin	Qazvin	36.26	50.02	14	1
Iran	Lorestan	Borujerd, 50KmSW	33.80	46.70	1	2
Iran	Kordestan	Aghbulagh Morched	35.62	48.66	7	2
Iran	Kordestan	Sanandaj, 32KmWNW	35.32	46.90	2	2
Iran	Kermanshah	Kermanshah	34.46	46.89	2	2
Iran	Hamedan	Malayer	34.08	49.08	4	2
Turkey	Adana	Adana	37.28	36.45	8	3
Turkey	Icel	Icel, Tarsous District	36.92	34.90	4	3
Turkey	Erzincan	Kara Dagh	39.65	39.10	1	a
Turkey	Izmir	Izmir	38.41	27.15	1	b
Iraq	Kirkuk	Kirkuk, Mullah abd Allah	35.35	44.45	1	c
Jordan	Irbid, Jaresh	Irbid, Jaresh	32.55	35.85	8	4

sides and perfect overlap at the level of the bullae, tooth rows and the orbital foramina on the lateral side were the criteria used to position the skulls. A scale was included in the images to allow the acquisition of a scaling factor for calculating centroid sizes (CS) (mm unit).

Only the left side of the skulls was digitized using TPSDIG 2.12 (Rohlf 2004). In total, 20, 19 and 21 two-dimensional (2D) landmarks were used on the ventral, dorsal and lateral sides of cranium, respectively (Fig. 2). Anatomical descriptions of the landmarks are based on the study by Popesko et al. (1992) and Tong (1989) (Appendix 3).

To minimize the inclusion of additional methodological errors, such as digitization and orientation errors, they were quantified and compared with the amount of natural variation in the sample. This was done on a subsample of specimens (10 intact skull of each taxon), following the procedure according to Adriaens (2007) (protocol available at http://www.fun-morph.ugent.be/Miscel/Methodology/Morphometrics.pdf). As the orientation error might be different depending on the view, the error testing was performed on the ventral, dorsal and lateral views, separately. The obtained mean of the digitization and orientation error for these views were very low (3% and 8% of the total variation, respectively).

We performed pooled analyses for intraspecific comparisons by pooling data from all three views, to get a full comprehension of shape variation in three dimensions (Monteiro et al. 2003). Still, species-specific differences proved to be very similar for the three views. As the ventral view included more taxonomically informative structures, only the visualization of shape differences in this view is included when summarizing the observations in this study. For the interspecific comparisons, only ventral skull data were included in the analyses.

As *a priori* criteria to assign specimens to the species studied involved aspects of auditory bulla morphology, which was also included in the shape data, the risk of circularity existed. As such, in addition to the analyses performed on the complete set of landmarks, we also performed an analysis on the ventral data set of all four species, but excluding the landmarks describing the bulla (LM 11–13). In case significant differences could be found between species, even after exclusion of these landmarks, this provided the guarantee that species-specific differences were not (only) based on criteria used for the *a priori* classification.

Data analysis

Shape analysis

A generalized Procrustes analysis (GPA) was performed using PAST (PAlaeontological STatistics) ver. 1.74 (Hammer et al. 2001) to separate size and shape variation (Rohlf and Slice 1990; Viscosi and Cardini 2011). For both the inter- and intraspecific comparison, principal component analyses (PCA, both standard and between-group) and CVA were performed on shape variables after the removal of redundant dimensions (due to the standardization through the GPA procedure), for which PAST and Statistica were used (STATSOFT, version 7.0, www.statsoft.com, StatSoft, Inc. 2004), respectively. The correlation between Procrustes shape distances and their corresponding Euclidean shape distances after projection in Euclidean shape space were tested using TpsSmall 1.20 (Rohlf 2003). For more details of this approach, see for example Viscosi and Cardini (2011).

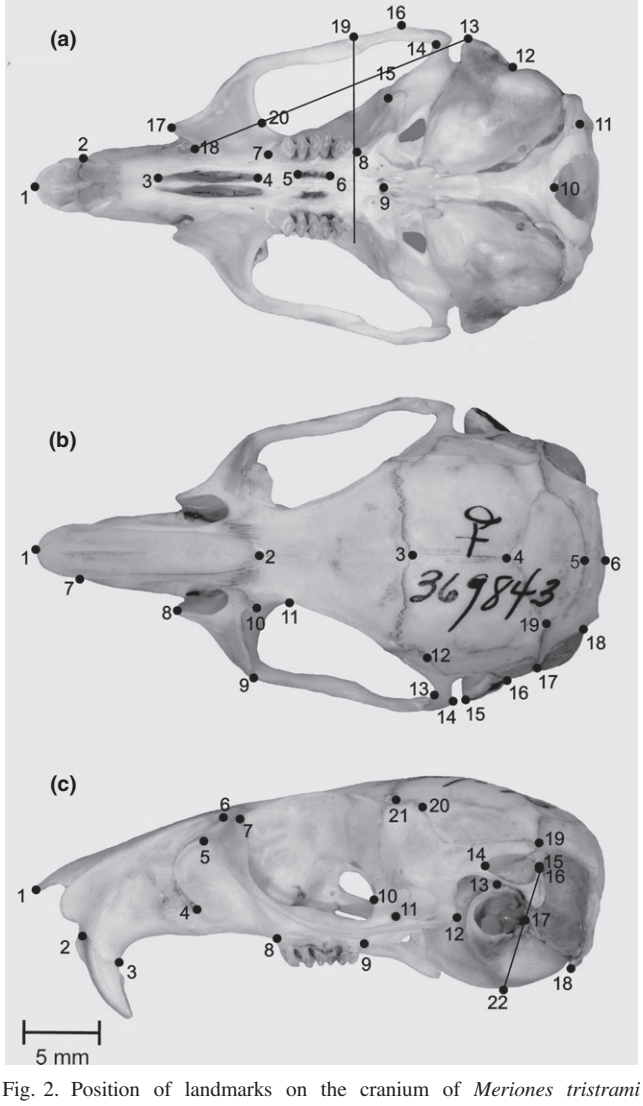

Fig. 2. Position of landmarks on the cranium of *Meriones tristrami* (specimen originating from Sanandaj, Iran) used in this study, shown in ventral (a), dorsal (b) and lateral view (c) (for a landmark description, see Appendix 3). The straight lines were used for defining the type III landmarks based on two other landmarks

However, for the interspecific data, some assumptions to perform parametric MANOVA with CVA were not met (data not normally distributed after performing multivariate normality test, no equivalence of covariance

after Box's M test and sample sizes not equivalent among the groups). Although the sensitivity of CVA's to these assumptions is highly discussed in the literature (see Kovarovic et al. 2011; Viscosi and Cardini 2011; Evin et al. 2013), we ran additional multivariate tests that provided insight into the reliability of these results, as well as tests that are not depending on these assumptions. First, CVA results were cross-validated using the leave-one-out procedure (Jack knife procedure) on the classifier matrix, where a concordance between classification success rates in the non-validated and validated analyses (obtained from the confusion matrix) indicates that group discrimination was not based on a one-case contribution. Second, a nonparametric MANOVA (NPMANOVA in past with 10 000 permutations, p-values Bonferroni corrected) was performed on the Euclidean distances in PAST, as well as a Monte Carlo randomization (10 000 permutations, p-values Bonferroni corrected) on Euclidean distances between group means using the POPTOOLS add-in (ver. 3.2.3) run under MICROSOFT OFFICE EXCEL 2007 (Hood 2010). To avoid overestimation of group differences (due to the deformation of the original shape space) in the CVA plots, scatter plots of a between-group PCA (BG-PCA) are provided here. The two-type specimens not included in the test for differences between groups were included in the PCA. For the interspecific comparison, the sample size for each of the groups was sufficiently high to allow a CVA on the full data set of shape variables (36 in total), where the smallest group size still exceeded well this number. As such, no data reduction was required and the analyses were run on all shape variables.

First, a complete assessment of interspecific differences was carried out on the pooled shape data of the ventral skull view (Adams 1999), with a NPMANOVA with Bonferroni-corrected p-values and 10 000 randomizations. Significance of pairwise differences among the *M. tristrami* groups (geoclimatical groups) was also tested by a Monte Carlo randomization (10 000 times randomization).

For the intraspecific comparison across *M. tristrami* groups, data were normally distributed but sample sizes were not equal, as well as the sample sizes were too low to allow further testing on all shape variables (also 36 in total). As such, a sensitivity analyses was performed in PAST to allow a reduction in variables without compromising the potential loss of relevant shape information (Rohlf and Slice 1990; Evin et al. 2013). For that, a CVA with confusion matrix calculation was performed on data sets comprising an increasing number of PC's (obtained from standard PCA on the original shape variables). The minimal number was defined by performing a broken stick analysis for significant PC's (being 4 for this data), and subsequent PC's were added and tested. Results converged between 15 and 16 PC's, so 16 PC's were included in the CVA analyses. The same analyses as for the interspecific comparison were performed (CVA with cross-validation, NPMANOVA with permutations, Monte Carlo randomization and between-group PCA), where for the nonparametric tests, the complete data set was used. All these analyses were run in PAST. In addition, we tried to quantify the amount of variation that explained the pairwise differences among each of the geoclimatical groups by performing a multivariate linear regression on shape data, using a dummy grouping variable (value of -1 and 1 for each of the group being compared). The R^2 values then provide and idea of the % variation explaining the difference between the pairs.

To visualize qualitatively how species (interspecific comparison) and geoclimatical groups within *M. tristrami* differed the most in skull shape, the BG-PCA scatter plots are provided but with CV1 manually superimposed on the data to allow a qualitative comparison between the BG-PCA plot and the CVA-derived wireframes (it is emphasized that this should then also be interpreted only in a qualitative manner). The first two PCA and CVA axes were used to generate deformed outline drawings using MORPHOJ (Klingenberg 2008). As both represented similar trends in shape variation, wireframe grids generated from CVA scores are given here. These are visual aids for highlighting regions in the skull that show the most variation, but where only the landmarks, relative within the complete landmark configuration, reflect actual shape variation (as such, the manually drawn outlines interconnecting landmarks are merely visual interpolations and should only be considered as such) (Klingenberg 2008; Viscosi and Cardini 2011).

Size analysis

Based on the scaled pictures, CS (Bookstein 1991) was calculated for the ventral cranium of all specimens of the four studied species using PAST. The assessment of the significance of interspecific size differences was carried out by an ANOVA using PAST. Pairwise comparisons of Euclidean distances (hence differences in absolute size) between the species and groups were performed using a Monte Carlo randomization, as mentioned above.

Results

Interspecific shape differences

The analyses on the ventral data set of all four species, of which landmarks demarcating the auditory bulla were excluded, confirmed that species were still significantly different from each other (NPMANOVA: $F = 214.4$, $p < 0.001$; Monte Carlo randomization $p < 0.001$). The *post hoc* test showed that all species, including species with a superficially very similar cranial morphology, are highly significantly different (Bonferroni-corrected $p < 0.0001$; Table 2). As such, circularity in the conclusions drawn further on can be excluded.

Looking at the ventral view data, *M. tristrami* and *M. persicus* overlap along the first two axes (Fig. 3a). Both CV1 and PC1 reflect the distinctness of *M. libycus* from the other species, which is characterized in having a relatively larger braincase and a more inflated tympanic bulla. The bulla in this species is protruded more rostrally and towards the zygomatic process of the squamous part of the temporal (relative shift of landmarks 13 with respect to 12) and the occiput is enlarged (Fig. 3b). Along PC2, *M. vinogradovi* lies largely isolated from the other species (completely separated for CV2), in having higher scores. Specimens of *M. libycus* and *M. persicus* have lower CV2 scores, with *M. tristrami* in between *M. persicus* and *M. vinogradovi*. The latter species shows a relatively narrower braincase (at the level of landmarks 12 and 13), a more widely flared zygomatic arches (landmarks 16 and 19 more laterally to the midline) and shorter and wider nasals (landmarks 1 and 2 closer to each other) (Fig. 3b). All tests showed that all four species differed significantly from each other (MANOVA $F_{108,1486} = 75.79$, $p < 0.0001$, similar classification success rates for non-validated and validated procedures; NPMANOVA $F = 214.4$, Bonferroni-corrected $p < 0.001$; Monte Carlo randomization $p < 0.001$).

Being highly distinct from the other species, *M. libycus* was not included in the further comparisons. In the analysis of the remaining species, CV1 mainly represents the same direction across the groups as PC2, separating *M. persicus* from *M. vinogradovi*, with *M. tristrami* lying in between and overlapping especially with *M. persicus* (Fig. 4a). However, CV2 does separate *M. tristrami* more from the other two than the BG-PC's do, indicating that it takes in a species-specific part of morphospace, as supported by the results from the MANOVA ($F_{72,554} = 36.96$, $p < 0.001$, similar classification success rates for non-validated and validated procedures), NPMANOVA ($F = 44.86$, $p < 0.001$) and Monte Carlo randomization ($p < 0.001$).

Table 2. Shape distances (Euclidean distances) between the species means (pairwise comparisons on the combined data of the three skull views)

Pairwise taxons	Euclidean distances between groups	*F*-value
Meriones tristrami–Meriones vinogradovi	0.029*	30
M. tristrami–Meriones persicus	0.026*	31
M. tristrami–Meriones libycus	0.060*	207
M. vinogradovi–M. persicus	0.042*	66
M. vinogradovi–M. libycus	0.070*	186
M. persicus–M. libycus	0.067*	490

*$p < 0.0001$.

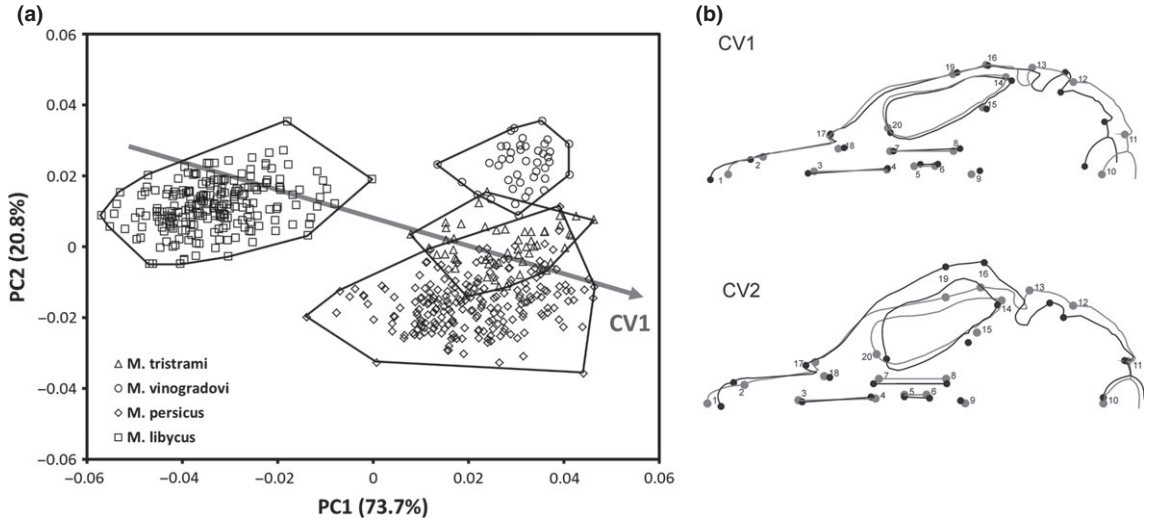

Fig. 3. Between-group principal component analyses (PCA) scatter plot (PC1 versus PC2) of the four studied *Meriones* species occurring in NE Iran (data based on ventral cranium). Outline drawings show the shape changes from the overall mean (in grey) to the shapes associated with the positive scores of the first two CV axes (in black). For better visibility, deformations were magnified two times. Percentage of between-group variance explained by the axes is given in parentheses

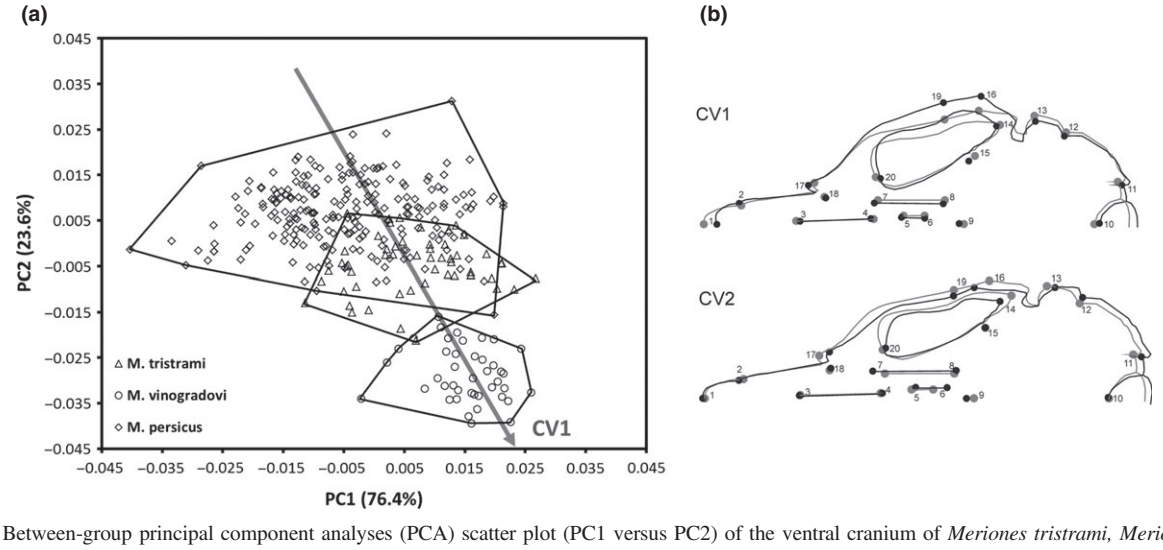

Fig. 4. Between-group principal component analyses (PCA) scatter plot (PC1 versus PC2) of the ventral cranium of *Meriones tristrami, Meriones persicus* and *Meriones vinogradovi* (data based on ventral cranium). Outline drawings show the shape changes from the overall mean (in grey) to the shapes associated with positive scores of the first two CV axes (in black). For better visibility, deformations were magnified two times. Percentage of between-group variance explained by the axes is given in parentheses

The CV1 and CV2 wireframes show that *M. tristrami* has a more laterally positioned zygomatic arch than *M. persicus* does, but more medial than in *M. vinogradovi* (Fig. 4b). It also shows an intermediate braincase width and a slightly shorter and more rostrally positioned palatine foramen, as well as the upper molar tooth row being slightly shorter with respect to the upper jaw (compared with both *M. persicus* and *M. vinogradovi*).

Interspecific size differences

The ANOVA revealed a highly significant difference between species ($F_{3,532} = 46.58$, $p < 0.0001$). Skull size in *Meriones tristrami* does not differ significantly from that of *M. persicus* and *M. vinogradovi*. The skull of *M. libycus*, on the other hand, is significantly larger than that of the other species (Table 3, Fig. 5).

Intraspecific shape differences in *Meriones tristrami*

The BG-PCA and CVA plots show that the skulls of both Iranian groups are similar, but that they both differ from those of Turkey and Jordan (Fig. 6). In the combined analyses on all views, all nonparametric tests confirmed this ($p \leq 0.001$ for comparisons between Iranian and non-Iranian populations), as well as that the two Iranian populations (Qazvin and western Iran) did not differ from each other and neither did the Turkish and Jordan ones ($p > 0.05$) (Table 4).

As the superimposed CV1 axes onto the BG-PCA plots for each of the individual views show, the Iranian groups are separated from the other two along this axis, especially for the ventral and lateral view ($p < 0.001$) ($p < 0.05$ for the dorsal view) (Fig. 6) (Table 4 for results on ventral view data). In a ventral view (Fig. 6a), the Iranian groups are characterized by a more

Table 3. Euclidean distances between the species centroid size means

Pairwise compared taxons	Euclidean distances between groups	p-value
Meriones tristrami–Meriones vinogradovi	1.7	0.0569
M. tristrami–Meriones persicus	1.3	0.056
M. tristrami–Meriones libycus	5.2	0.0001
M. vinogradovi–M. persicus	0.4	0.5698
M. vinogradovi–M. libycus	3.4	0.0001
M. persicus–M. libycus	3.9	0.0001

p-values obtained from the Monte Carlo randomization test.

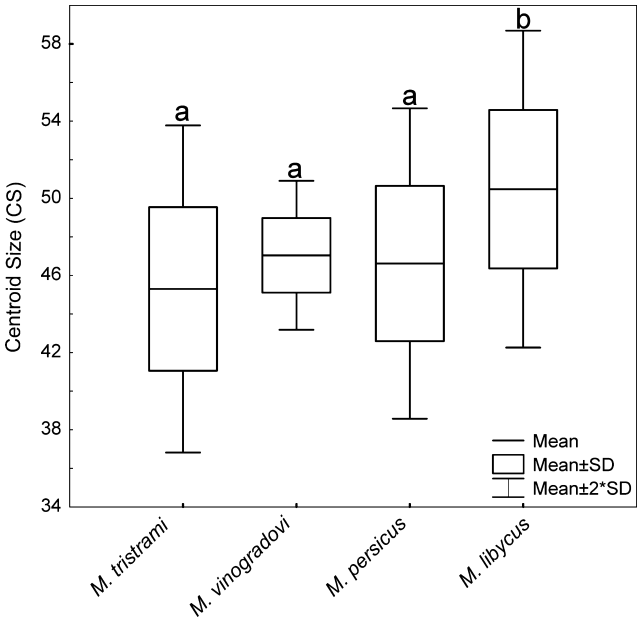

Fig. 5. Box-and-whisker plot showing the interspecific difference and ranges in centroid size of the ventral cranium. Boxes with different letters indicate a significant difference in size

Table 4. Shape distances (based upon Euclidean distances) between the *Meriones tristrami* groups mean

Pairwise grouping	Ventral	Dorsal	Lateral
Qazvin–West Iran	0.0131	0.0105	0.0139
Qazvin–Turkey	0.0235**	0.0194*	0.0218*
Qazvin–Jordan	0.0272**	0.0190**	0.0265**
West Iran–Turkey	0.0256**	0.0209**	0.0249**
West Iran–Jordan	0.0268**	0.0206*	0.0285**
Turkey–Jordan	0.0094	0.0126	0.0177

Bonferroni-corrected p-levels obtained from the Monte Carlo randomization test – *$p < 0.01$, **$p < 0.001$.

laterally extended zygomatic arch (landmarks 16 and 19 positioned further away from the midline), a shorter occiput (space in between landmarks 8–11 smaller), broader maxilla (landmarks 17 and 18 wider apart from each other), slightly shorter tooth row (landmarks 7 and 8 closer to each other) and elongated nasals (landmarks 1 and 2 wider apart). For the dorsal shape (Fig. 6b), the Iranian groups have a slightly wider skull at the level of the zygoma (landmarks 9, 13 and 14 more distant from the midline) and shorter occiput (landmarks 5 and 6 substantially closer to landmark 4). For the lateral shape (Fig. 6c), where the Jordan and Turkish group lie separated from each other (although are not significantly different, NPMANOVA: $p > 0.05$), the Iranian groups are characterized in having a slightly higher nasal region (landmarks 1, 2 and 3 more spread out), zygomatic process of squamous part of temporal bone situated more caudally (landmarks 12 and 17 closer to each other) and a less inflated tympanic bulla (landmarks 17, 18 and 22 closer to each other).

Looking at the amount of variance that explains the pairwise differences between these groups, there seems to be a relation with the distinctiveness among the groups to some degree. Lowest levels of explained variance are found between the Turkish and Jordan group (between 4.8% and 6.3%, depending on the view) and between the two Iranian groups (between 4.1% and 7.6%). Highest levels are found between the Jordan group and both the Iranian ones (between 13.3% and 27.6%). Although the Jordan and Turkish group were separated in the PCA scatter plot of the lateral view data (PC1 versus PC2, Fig. 6c), the variance explained between them is lower for the lateral view data than for the dorsal one (6.3% versus 9.5%).

Size differences between the *Meriones tristrami* groups

In both Iranian groups, the average skull is larger than in the other groups, although not significantly. But, western Iran skulls are significantly larger than those of Turkey and Jordan ($0.01 < p < 0.05$), as well as those of the Qazvin group ($0.0001 < p < 0.0005$). The Jordan group has the smallest cranium on average, although not significantly different from that of the specimens from Turkey (Fig. 7).

Discussion and conclusion

The results corroborate what has already been suggested by, for example, Osborne and Helmy (1980), Harrison (1991), Yiğit and Çolak (1999) and Darvish (2009), confirming that in Iran, sympatrically occurring *Meriones* species, *M. libycus, M. persicus, M. vinogradovi* and *M. tristrami,* are morphologically distinct. *Meriones libycus* is clearly most distinct from this cluster, mainly due to the relatively larger tympanic bulla. Patterns of variation in bulla size have been described for other species, but also occur at an intraspecific level as observed in *Meriones meridianus* (Tabatabaei Yazdi et al. 2012). It has been claimed that this could reflect differences in climatological conditions, where living in xeric environments has been associated with a larger bullae and may even have an impact on hearing performance (Harrison 1972; Vaughan et al. 2000). Our results also confirm that phenotypic differences between the latter three species are more subtle. However, they do allow us to reject the hypothesis that there would be no significant difference in the phenotypic range of the skull shape. Differences were found to be particularly pronounced at the level of the zygomatic arch and the nasal.

The taxonomy of *Meriones* is complicated, as is the assessment of diagnostic morphological differences, taking into consideration the level of intraspecific variation. Indeed, Struhsaker (1981) warned that morphological comparisons of skulls to define diagnostic criteria might be hampered by the remarkable morphological variation within the species. This study does corroborate the presence of a large amount of intraspecific variation (looking at the spreading of group-specific PC scores), with a substantial overlap in morphospace of at least three of these sympatric *Meriones* species studied, that is, *M. tristrami, M. persicus* and *M. vinogradovi* (and especially between the former 2).

Our results clearly show that there is statistical support for a discrimination of all four species based on their skull shape and size. However, going from this information, based on multivariate

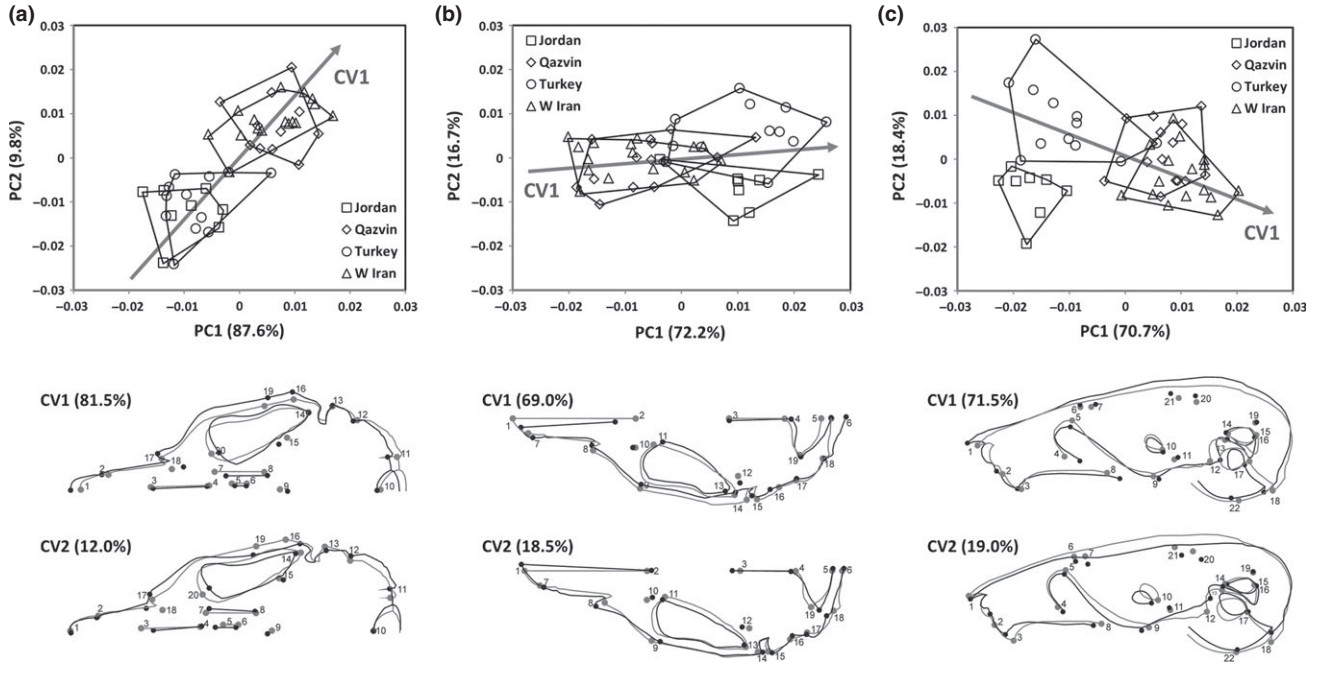

Fig. 6. Between-group principal component analyses (PCA) scatter plots (PC1 versus PC2) based on shape data of the ventral (a), dorsal (b) and lateral (c) views of the skull in the *Meriones tristrami* groups. Outline drawings show the shape changes from the overall mean (in grey) associated with positive scores of the first two CV axes (in black). For better visibility, deformations were magnified three times. Percentage of between-group variance explained by the axes is given in parentheses

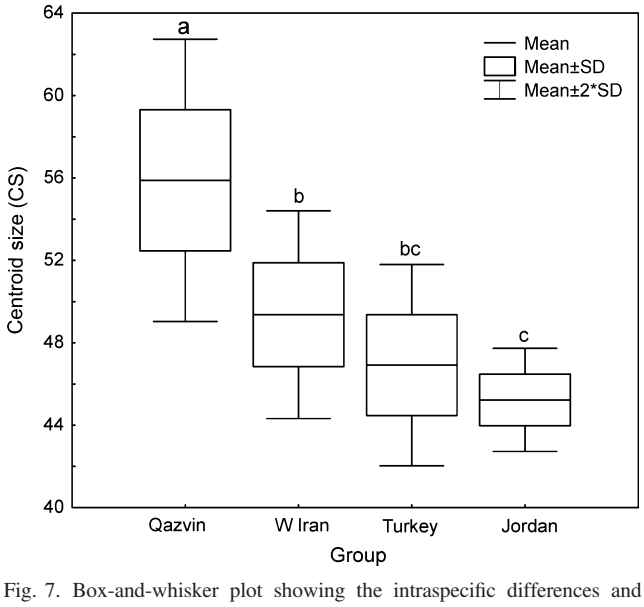

Fig. 7. Box-and-whisker plot showing the intraspecific differences and ranges across *Meriones tristrami* groups of centroid size of the ventral cranium in four groups of *M. tristrami*. Boxes with different letters indicate a significant difference in size (p-level: 0.05)

shape and size data, towards constructing diagnostic features for species discrimination, in a manner that is practically user-friendly, is a whole other matter. Suitable keys depend on the amount of intraspecific variation that has been considered when defining discriminative characters (Dobigny et al. 2002; Denys et al. 2003; Cordeiro-Estrela et al. 2008). This is especially crucial when dealing with subtle levels of interspecific variation that hardly surpass the intraspecific one. This becomes especially problematic when it involves species that co-occur, so that geographical origin cannot be used as a criterion, as is the case for *M. tristrami, M. persicus and M. vinogradovi* (Misonne 1959; Harrison 1991; Yiğit and Çolak 1999). Based on our analysis, incorporating morphologies from a wide geographical range could thus provide a solid base for extracting usable and reliable diagnostic traits that can be implemented into identification keys of *Meriones*. Objective classification methods of a continuous range of shape variation would here be very useful, still this remains a challenge for taxonomical research. Several tools have been developed for automated quality assessment and cultivar classification of shapes for agricultural and other industrial applications (for a review, see Costa et al. 2011). These approaches could be equally applicable to discriminate between morphotypes, and hence between species. Although classification methods, where specimens are assigned to *a priori* defined classes (such as species, populations) based on best fit (similar to classifications for a CVA validation, or partial least squares discriminant analysis) (Menesatti et al. 2008), it could be more interesting to apply a more open approach of modelling where specimens could be put in a new, yet undefined class, in case it would not fit in the predefined ones. This could allow a more efficient recognition of outliers, which may or may not allow to identify new natural groups.

Confirming Misonne (1975), our study supports the hypothesis that Iranian specimens of *M. tristrami*, occupying its most eastern geographical range, are indeed phenotypically distinct from those from other parts of its distribution range, such as Turkey and Jordan. Similarly, Yiğit et al. (1998) observed phenotypic differences in specimens originating from south-eastern and eastern Anatolia. These differences formed the base for assigning them to a new subspecies, *M. t. bogdanovi* Heptner, 1931 (Type locality: Saljany district eastern Transcaucasia), in that way distinguishing them from the existing *M. t. lycaon* Thomas, 1919 (Type locality: Karadag, Turkey). However, as in the latter study, no specimens were included from Iran, the validity of these subspecies could become doubtful based on what our results show. Considering the distinctiveness of these Iranian populations, the taxonomic structure (and substructure at subspecies level) could

be more complex than anticipated. Considering that the northwest of the Iranian plateau is one of the most complex zoogeographical regions within the Palearctic region, cryptic diversity could be expected to be high (Anderson1989; Firouz 2005). Nevertheless, it is highly questionable whether geometric morphometrics and skull data could solve this problem.

The morphometric data here thus show that geographical differences in skull shape exist in *M. tristrami*. The question remaining to be solved then is to what degree this reflects diverging morphologies due to reproductive isolation, and hence speciation, or whether this reflects local adaptations to a different environment, or even non-adaptive patterns of morphological variation (e.g. resulting from genetic drift). Testing hypotheses on adaptive explanations of subtle shape differences has a conceptual framework, following the paradigm of Arnold (1983). Still, designing experiments to test the correlation between shape variation and performance can be difficult, especially when subtle changes are situated in parts of the skull that are seemingly non-functional units (e.g. the observed variation in the shape of the nasal bones, and the position and size of the palatine fissure). Other features then do suggest implications on performance, such as a more lateral zygomatic arch, which can provide more space for jaw adductor muscles (Van Daele et al. 2009). Variation observed in the upper jaw can be related to subtle differences in the use of the upper incisors when manipulating food that shows differences in hardness, as well as different patterns in size-related scaling effects in the procumbency of these teeth (as found in rodents that use their teeth to dig) (Mora et al. 2003). As mentioned earlier, also the size and shape of the auditory bulla may reflect adaptations related to vocal communication. Still, these all involve hypotheses that require a functional morphological testing.

Although this study provides some contribution to a further clarification of the taxonomy of the jird species, and hence a better understanding of the biodiversity in the Middle East, still much needs to be explored. The fauna of this region, and especially Iran, is a poorly studied, even when compared to its neighbouring countries such as Turkey.

Acknowledgements

We are very grateful to all museum curators and collection managers who provided us with access to the collections. The suggestions of two anonymous reviewers, as well as of Andrea Cardini and Philip Cox greatly improved the manuscript.

References

Adams DC (1999) Methods for shape analysis of landmark data from articulated structures. Evol Ecol Res **1**:959–970.

Adams DC, Slice DE, Rohlf FJ (2004) Geometric morphometrics: ten years of progress following the 'revolution'. Ital J Zool **71**:5–16.

Adriaens D (2007) Protocol for error testing in landmark based geometric zrmorphometrics. http://www.fun-morph.ugent.be/Miscel/Methodology/Morphometrics.pdf.

Anderson SC (1989) Fauna of Persia. In: Yarshater E (ed.), Encyclopedia Iranica Volume 9, pp 437–446. Bibliotheca Persica Press, New York, USA. 672p.

Arnold SJ (1983) Morphology, performance and fitness. Am Zool **23**:347–361.

Barciova L, Macholán M (2006) Morphometric study of two species of wood mice *Apodemus sylvaticus* and *A. flavicollis* (Rodentia: Muridae): traditional and geometric morphometric approach. Acta Theriol **51**:15–27.

Benazzou T (1984) Contribution à l'étude chromosomique et de la diversification biochimiuque des Gerbillidés (Rongeurs). Ph.D. Thesis, Université de Paris XI, Paris, France.

Bookstein FL (1991) Morphometric Tools for Landmark Data. Cambridge University Press, New York, pp 1–435.

Cardini A, Elton S (2009) The radiation of red colobus monkeys (Primates, Colobinae): morphological evolution in a clade of endangered African primates. Zool J Linn Soc Lond **157**:197–224.

Cardini A, Jansson A-U, Elton S (2007) Ecomorphology of vervet monkeys: a geometric morphometric approach to the study of clinical variation. J Biogeogr **34**:1663–1678.

Chaworth-Musters JL, Ellerman JR (1947) A revision of the genus *Meriones*. Proc Zool Soc Lond A **117**:478–504.

Chevret P, Dobigny G (2005) Systematics and evolution of the subfamily Gerbillinae (Mammalia, Rodentia, Muridae). Mol Phylogenet Evol **35**:674–688.

Cordeiro-Estrela P, Baylac M, Denys C, Polop J (2008) Combining geometric morphometrics and pattern recognition to identify interspecific patterns of skull variation: case study in sympatric Argentinian species of the genus *Calomys* (Rodentia: Cricetidae: Sigmodontinae). Biol J Linn Soc **94**:365–378.

Coşkun Y (1999) Diyarbakõr *Meriones tristrami* Thomas, 1892 (Mammalia: Gerbillinae) Türünün Morfolojik Özellikleri. Turk J Zool **23**:345–355.

Costa C, Antonucci F, Pallottino F, Aguzzi J, Sun DW, Menesatti P (2011) Shape analysis of agricultural products: a review of recent research advances and potential application to computer vision. Food Bioprocess Technol **4**:673–692.

Darvish J (2009) Morphometric comparison of fourteen species of the genus *Meriones* Illiger, 1811 (Gerbillinae, Rodentia) from Asia and North Africa. Iran J Anim Biosyst **5**:59–77.

Darvish J (2011) Morphological comparison of fourteen species of the genus *Meriones* Illiger, 1811 (Gerbillinae, Rodentia) from Asia and North Africa. Iran J Anim Biosyst **7**:50–72.

Demirbaş Y, Pamukoğlu N (2008) The bioecology of *Meriones tristrami* Thomas, 1892 in Kõrõkkale Province (Mammalia: Rodentia). Int J Nat Eng Sci **2**:39–44.

Denys C, Lecompte E, Granjon L, Baylac M, Cordeiro P, Cornette R, Dobigny G, Fichet-Calvet E, Hugot JP, Meslage C, Millien-Parra V, Petrillo P, Volobouev V, Welz M (2003) Integrative systematics: the importance of combining various techniques for increasing knowledge of African Murinae. In: Singleton GR, Hinds LA, Krebs CJ, Spratt DM (eds). Rats, mice and people: rodent biology and management. ACIAR, Canberra, pp 499–506.

Dobigny G, Baylac M, Denys C (2002) Geometric morphometrics, neural networks and diagnosis of sibling *Taterillus* (Rodentia, Gerbillinae) species. Biol J Linn Soc **77**:319–327.

Evin A, Cucchi T, Cardini A, Vidarsdottir US, Larson G, Dobney K (2013) The long and winding road: identifying pig domestication through molar size and shape. J Archaeol Sci **40**:735–743.

Fadda C, Corti M (2000) Three-dimensional geometric morphometrics of *Arvicanthis*: implications for systematics and taxonomy. J Zool Syst Evol Res **39**:235–245.

Firouz S (2005) The Complete Fauna of Iran. I B Tauris Publishers, London, pp 1–322.

Hammer Ø, Harper DAT, Ryan PD (2001) PAST: paleontological statistics software package for education and data analysis. Palaeontol Electronica **4**:1–9.

Harrison DL (1972) The Mammals of Arabia. 3. Lagomorpha and Rodentia. Benn, London, pp 382–670.

Harrison DL, Bates PJJ (1991) The Mammals of Arabia, 2nd edn. Harrison Zoological Museum Pub, pp 1–354.

Hood GM (2010) PopTools version 3.2.3. Available on the internet. URL http://www.Poptools.org.

Karami M, Hutterer R, Benda P, Siahsarvie R, Kryštufek B (2008) Annotated check-list of the mammals of Iran. Lynx (Praha) **39**:63–102.

Klingenberg CP (2008) MorphoJ. Faculty of Life Sciences, University of Manchester, UK. Available at http://www.flywings.org.uk/MorphoJ-page.htm

Kovarovic K, Aiello LC, Cardini A, Lockwood CA (2011) Discriminant function analyses in archaeology: are classification rates too good to be true? J Archaeol Sci **38**:3006–3018.

Lay DM (1967) A study of the mammals of Iran, resulting from the Street Expedition of 1962–63. Fieldiana Zool **54**:1–282.

Macholàn M, Mikula O, Vohralik V (2008) Geographic phenetic variation of two eastern-Mediterranean non-commensal mouse species, *Mus macedonicus* and *M. cypriacus* (Rodentia: Muridae) based on traditional and geometric approaches to morphometrics. Zool Anz **247**:67–80.

Menesatti P, Costa C, Paglia G, Pallottino F, D'Andrea S, Rimatori V, Aguzzi J (2008) Shape-based methodology for multivariate discrimination among Italian hazelnut cultivars. Biosyst Eng **101**:417–424.

Misonne X (1957) Mammiferes de la Turquie Sub-orientale et du nord de la Syrie. Mammalia **21**:53–68.

Misonne X (1959) Analyse Zoogéographique des mammifères de l'Iran. Mem Inst Roy Sci Nat Belgique, Bruxelles 2nd Ser **59**: pp 1–157.

Misonne X (1975) The rodents of the Iranian deserts. In: Prakash I, Ghosh PK (eds), Rodents in Desert Environments, Junk W, The Hague, pp 47–58.

Monteiro LR, Duarte LC, dos Reis SF (2003) Environmental correlates of geographical variation in skull and mandible shape of *Thrichomys apereoides* (Rodentia: Echimyidae). J Zool **261**:47–57.

Mora M, Olivares AI, Vassallo AI (2003) Size, shape and structural versatility of the skull of the subterranean rodent *Ctenomys* (Rodentia, Caviomorpha): functional and morphological analysis. Biol J Linn Soc **78**:85–96.

Musser GG, Carleton MD (2005) Superfamily Muroidea. pp 894-1531. In: Wilson DE, Reeder DM (eds), Mammal Species of the World: A Taxonomic and Geographic Reference, 3rd edn. Johns Hopkins University Press, Baltimore, MD, pp 745–2142.

Naseri CZ, Jalal R, Darvish J, Farsi M (2006) Determination of *Meriones* Species (Rodentia, Gerbillinae) by RAPD-PCR. Iran J Anim Biosyst **2**:35–40.

Osborne DJ, Helmy I (1980) The contemporary land mammals of Egypt (including Sinai). Fieldiana Zool, New Series **5**:1–579.

Pavlinov IY (2008) A Review of Phylogeny and Classification of Gerbillinae (*Mammalia*: *Rodentia*). Moscow Univ Publ, Moscow, pp 68.

Petter F (1959) Evolution du dessin de la surface d'usure des molaires des *Gerbillidés*. Mammalia **23**:304–315.

Popesko P, Rajtovà V, Horàk J (1992) Colour Atlas of the Anatomy of Small Laboratory Animals, Vol. 2, Rat, Mouse and Golden Hamster. Wolfe Publishing, Bratislava, pp 1–253.

Rohlf FJ (2004) TpsDig: Thin Plate Spline Digitise. Department of Ecology and Evolution, State University of New York, Stony Brook, New York. Available at http://life.bio.sunysb.edu/morph/.

Rohlf FJ (2003) TpsSmall: Thin Plate Spline Small Variation Analysis. Stony Brook, New York: Departement of Ecology and Evolution, State University of New York. Available at http://life.bio.sunysb.edu/morph/.

Rohlf FJ, Marcus LF (1993) A revolution in morphometrics. Trends Ecol Evol **8**:129–132.

Rohlf FJ, Slice DE (1990) Extensions of the Procrustes method for the optimal superimposition of landmarks. Syst Zool **39**:40–59.

StatSoft, Inc. (2004) STATISTICA (Data Analysis Software System), Version 7. StatSoft, Inc., Tulsa, OK. www.statsoft.com.

Struhsaker TT (1981) Vocalizations, phylogeny and palaeogeography of red colobus Monkeys (*Colobus badius*). Afr J Ecol **19**:265–283.

Tabatabaei Yazdi F, Adriaens D, Darvish J (2012) Geographic pattern of cranial differentiation in the Asian Midday Jird *Meriones meridianus* (Rodentia: Muridae: Gerbillinae) and its taxonomic implications. J Zool Syst Evol Res **50**:157–164.

Thomas O (1892) On a new species of Meriones. Ann Mag Nat Hist **9**:147–149.

Tong H (1989) Origine et évolution des Gerbillidae (Mammalia, Rodentia) en Afrique Du Nord. Mem Soc Geol France **155**:1–120.

Van Daele P, Herrel A, Adriaens D (2009) Biting performance in teeth-digging African mole-rats (Fukomys, Bathyergidae, Rodentia). Physiol Biochem Zool **82**:40–50.

Vaughan TA, Ryan JM, Czaplewski NJ (2000) Mammalogy, 4th edn. Saunders College Publishers, Orland, FL, pp 1–565.

Viscosi V, Cardini A (2011) Leaves, taxonomy and geometric morphometrics: a simplified protocol for beginners. PLoS ONE **6**:e25630.

Yiğit N, Çolak E (1998) A new subspecies of *Meriones tristrami* Thomas, 1892 (Mammalia: Gerbillinae) from kilis (Southeastern Turkey): *Meriones tristrami kilisensis* subsp. N Turk J Zool **22**:99–103.

Yiğit N, Çolak E (1999) A study of the taxonomy and karyology of *Meriones persicus* (Blanford, 1875) (Mammalia: Rodentia) in Turkey. Turk J Zool **23**:269–274.

Yiğit N, Çolak E, Özkurt Ş (1995) Biology of *Meriones tristrami* Thomas, 1892 (Rodentia: Gerbillinae) in Turkey. N Turk J Zool **19**:337–341.

Yiğit N, Kõvanç E, Çolak E (1998) Taxonomic Status of *Meriones tristrami* Thomas, 1892 (Rodentia: Gerbillinae) in Turkey. Zoology in the Middle East **16**:19–30.

Yiğit N, Çolak E, Sözen M, Özkurt Ş (1999) *Meriones tristrami* Thomas, 1892 (Mammalia: Rodentia)'nin Diş Gelişimi, Diş Aşõnõmõ ve Yaş Tayini. N Turk J Zool **23**:965–971.

Yiğit N, Gharkheloo MM, Çolak E, Özkurt S, Bulut S, Kankiliç T, Çolak R (2006) The karyotypes of some rodent species (Mammalia: Rodentia) from eastern Turkey and northern Iran with a new record, *Microtus schidlovskii* Argyropulo, 1933, from eastern Turkey. N Turk J Zool **30**:459–464.

Appendix 1. List of the analysed specimens

Meriones libycus

Smithsonian Natural Museum of Natural History (Washington, DC, USA)

326941, 326942, 326943, 326944, 326969, 326970, 326971, 326973, 328266, 328267, 328269, 369798, 369799, 369801, 369802, 369806, 369808, 369810, 369812, 369814, 369815, 369817, 369818, 369819, 369822, 369824, 369826, 369827, 369828, 369829, 369831, 369832, 369833, 369834, 354682, 326968, 328257, 328258, 328260, 328262, 328264, 328265, 354690, 354691, 354692, 354695, 341256, 341258, 341261, 341262, 341263, 341264, 341265, 341266, 341267, 328224, 328225, 328271, 328272, 328273, 328274, 328275, 329188, 329189, 329190, 329191, 354696, 354661, 350558, 350559, 350572, 354647, 354649, 354650, 354652, 354653, 354664, 354665.

British Museum of Natural History (London, UK)

40.259, 1983.314, 40.257, 25.4.3.43, 25.4.3.23, 10.3.12.4, 25.4.3.25, 5.7.2.3, 25.4.3.20, 47.383, 56.2.29.5, 19.12.10.3, 47.1412, 47.1414.

Zoological Museum of Ferdowsi University of Mashhad (Mashhad, Iran)

M564, M799, M810, M785, 322, 245, M-35, 1021, 30, 1499, 909, 1473, 1504, 303, 208, 474, 1470, 1468, M844, M571, 1506, 1471, 217, M-17, M-35, 157, M-3, 39, M-28, M-36, 205, 212, M-21, 174, M-29, 1469, 24, M-34, M-7, 518, M-37, 176, 563, M-1, 1482, 574, 461, 88, 9, M-572, M-579, M-12, M-808, 4, M-432, M343, 2, M-331, M-188, M-646, M-196, M-11, 850, 11, M-111, M-842, M-573, 7, M-175, M-548, 14, M-694, M-568, M-236, M-251, 840, 577, 106, M-3, M-12.

Musée National d'Histoire Naturelle (Paris, France)

1950.468, 1950.508, 1957.1330, 1957.1338, 1957.1339, 1958.89, 1958.91, 1958.330, 1958.331, 1958.336, 1958.341, 1958342, 1958343, 1958.344, 1958.345, 1958.346, 1958.347, 1958.351, 1958.352, 1958.750, 1957-334, 1957-335, 1957-332, 1957-336.

Royal Belgian Institute of Natural Sciences (Brussels, Belgium)

10186, 10190, 10189, 10187, 10348, 10322, 10192, 10078, 10137, 10283, 10184, 10497, 10185, 10188, 10318, 10319, 10082, 10282, 10194.

Appendix 1. (Continued)

Meriones tristrami

Smithsonian Natural Museum of Natural History (Washington, DC, USA)

369843, 350513, 327435, 327436, 327437, 327438.

Field Museum of Natural History (Chicago, IL, USA)

181370, 97383, 97384, 97385, 112123, 112124, 112125, 112126, 112115, 112116, 112122, 97379, 97381, 97386, 97387, 97389, 97390, 97391, 111952, 179029, 179030, 179031, 179032, 179034, 179035, 179036, 179037, 122288, 122289, 122290, 122295, 122297, 122300, 122306, 122303, 97383.

Musée National d'Histoire Naturelle (Paris, France)

1957-299, 1957-1371, 1957-1381, 1957-1373, 1957-1390, 1957-1380, 1957-1393, 1957-1395, 1957-1396, 1957-1399, 1957-1401, 1957-1406.

British Museum of Natural History (London, UK)

8.7.1.28: Type of *Meriones blacklery lycaon* (*M. t. lycaon*) and 3.6.1.1: Type of *Meriones blackleri* (*M. t. blackleri*).

Meriones persicus

Smithsonian Natural Museum of Natural History (Washington, DC, USA)

354661, 350558, 350559, 350572, 354647, 354649, 354650, 354652, 354653, 354664, 354665, 326875, 326876, 326877, 326879, 326880, 326881, 326882, 326884, 326885, 326886, 326887, 326890, 326892, 326894, 326895, 326896, 326897, 326898, 326903, 341248, 350560, 350562, 350563, 350564, 350565, 350566, 350568, 350570, 350571, 341249, 341251, 354654, 354655, 354656, 354657, 354658, 354659, 328336, 328337, 328338, 329181, 353657, 353658, 353659, 353660, 353684, 353695, 353696, 353697, 353698, 411090, 411091, 411093, 411094, 413607, 413608, 411087.

Field Museum of Natural History (Chicago, IL, USA)

97295, 97290, 97314, 57896, 57899, 57289, 57290, 57295, 57298, 97300, 97303, 97304, 97305, 97309, 97313, 97314, 97342, 97343, 97347, 97349, 84508, 111801, 111940, 111944, 111945, 111951, 111953, 111964, 111998, 112003, 112034, 112035, 103500, 103503, 103505, 103507, 103508, 103397, 103398, 103399, 103402, 103403, 103404, 103405, 103485, 103486, 103487, 103523, 103524, 103525, 103526, 103527, 84464, 97358, 97360, 111968, 111982, 111986, 111989, 111992, 111979, 11980, 11982, 112021, 112023.

British Museum of Natural History (London, UK)

77.3052, 20.5.20.3, 20.2.9.21, 19.11.8.42, 19.11.7.72, 71.1581, 16.11.7.68, 19.11.7.71, 70.20.24, 70.20.23.

Zoological Museum of Ferdowsi University of Mashhad (Mashhad, Iran)

1399, 10, 14, 1396, 6, 1394, 28, 1395, 22, 24, 1397, 11, 27, 18, 8, 498, 135, 18, 333, 1392, 655, M-18, 566, 114, 320, 321, 315, M-15, 317, M-1111, M-1116, M-1113, M-1115, M-1110, M-110, 1571, M-1114, 1112, M560, 1398.

Musée National d'Histoire Naturelle (Paris, France)

1947.846, 1947.848, 1950.419, 1950.420, 1950.421, 1950.430, 1950.431, 1957.978, 1957.993, 1985.1628, 1991.241, 1957-290, 1957-203, 1957-257, 1957-200, 1957-221, 1957-285, 1957-245, 1957-215, 1957-226, 1957-234, 1957-273, 1957-186, 1957-983, 1957-209, 1957-272, 1957-210, 1957-283, 1957-229, 1957-223, 1957-246, 1957-227, 1957-231, 1957-232, 1957-190.

Royal Belgian Institute of Natural Sciences (Brussels, Belgium)

10498, 10369, 10072, 10363, 10051, 10427, 10365, 10034, 10043, 10370, 10038, 10425, 10026, 10366, 10041, 10039, 10361, 10368, 10025, 10042, 10044, 9884, 10377, 10364, 10379, 10032, 10074, 10064, 10373, 10031.

Meriones vinogradovi

Smithsonian Natural Museum of Natural History (Washington, DC, USA)

354662, 354663.

Field Museum of Natural History (Chicago, IL, USA)

97395, 97396, 97399, 97400, 97401, 97402, 97403, 97404, 97405, 97406, 97409, 97410, 97407, 97408.

Musée National d'Histoire Naturelle (Paris, France)

1950.459, 1950.468, 1950.476, 1950.477, 1950.478, 1950.481, 1953.426, 1957.522, 1958.265, 1985.1627, 1985.1630.

Royal Belgian Institute of Natural Sciences (Brussels, Belgium)

10179, 10417, 9895, 10493, 9890, 9893, 10320, 9885, 9897, 9891, 10278, 10277, 10274, 10411, 9898, 9886, 9888, 10273, 10423, 10419, 9894, 10279.

Appendix 2. Sampling localities of the examined specimens, *Meriones libycus*, *Meriones persicus* and *Meriones vinogradivi*

Meriones persicus

Country	Province	Specific locality	Lat.	Lon.	Sample ize
Iran	Chahar mahal and Bakhtiari	Kuh rang, Lordegan	32.351N	50.156E	3
	East Azarbaijan	Miyaneh	37.433N	47.155E	4
	East Azarbaijan	Sarab	37.926N	47.548E	1
	East Azarbaijan	Kouhak (Kohak Darrehsō?)	37.578N	46.284E	1
	Esfahan	Sarvestan	33.133N	51.818E	1
	Fars	Yasuj	30.595N	51.500E	14
	Golestan	Dasht, Dashliboroon, Torkman sahra	37.633N	54.817E	2
	Hamedan	Hamedan	35.700N	48.200E	3
	Hormozgan	Geno	27.417N	56.183E	11
	Ilam	Ilam	33.638N	46.431E	19
	Kerman	Kerman	29.900N	56.533E	3
	Kermanshah	Asadabad	37.766N	48.116E	2
	Kermanshah	Qhasr e shirin	34.318N	47.087E	1
	Kermanshah	Sameleh	34.021N	47.307E	5
	Khorasan	Birjand	32.867N	59.200E	3
	Khorasan	Bojnord	37.467N	57.317E	3
	Khorasan	Gonbad-e-Kavus	37.233N	55.083E	1
	Khorasan	Khajar	35.100N	54.700E	11
	Khorasan	Kashmar, Duruna, Bardaskan (kavir-e-Namak)	35.183N	57.415E	1
	Khorasan	Mashhad	36.267N	61.050E	1
	Khorasan	Tandureh	37.383N	58.833E	6
	Khorasan	Torbatheidariyeh, Rushkar, Sangan, Jangal, Isfadeh, Maehneh	35.283N	59.217E	7
	Khorasan (Razavi)	Bajestan	34.517N	58.183E	1
	Khuzestan	Behbahan	30.598N	50.245E	4
	Khuzestan	Masjed soleiman+	31.933N	49.300E	8
	Kordestan	Aghbulagh Morshed	35.620N	48.660E	2
	Kordestan	Sanandaj, Bijar, Marivan	35.310N	46.999E	6
	Kordestan	Saghez	36.241N	46.268E	1
	Lorestan	Khorram abad	33.491N	48.333E	7
	Markazi	Mahallat	33.750N	50.500E	2
	Mazandaran	Noshahr (Sama)	36.480N	51.338E	5
	Qazvin	Qazvin	36.267N	50.017E	19
	Sistan va Baluchestan	Khash	28.250N	61.200E	3
	Sistan va Baluchestan	Zahedan	29.217N	60.867E	1
	Tehran	Tehran	35.850N	50.867E	8
	West Azarbaijan	Naghadeh	36.933N	45.367E	3
	West Azarbaijan	Rezaeieh, Makoo	37.491N	44.99E	10
	Zanjan	Soltanieh	36.454N	48.799E	1
	Zanjan	Zanjan	36.683N	48.487E	1
Afghanistan	Bamyan	Bamyan	34.817N	67.879E	5
	Herat	Herat, 8 mi N	34.449N	62.167E	6
	Kabol	Paghman	34.583N	68.950E	3
	Kandahar	Kandahar, 4 mi N	31.658N	65.783E	5
Pakistan	Baluchistan	Quetta Division, Urak Valley	30.360N	67.020E	14
	Punjab	Dera Ghazi Khan Division	30.050N	70.633E	1
Iraq	Sulaymaniyah	Penjwin	35.617N	47.000E	2

Meriones vinogradovi

Country	Specific loc.	Abbreviation	Lat.	Lon.	Sample size
Iran	East Azarbaijan, Jolfa	JLF	38.917N	45.500E	9
Iran	Kordestan, Aghbulagh	AGH	35.610N	48.120E	12
Iran	Qazvin	QZV	36.267N	50.017E	10
Iran	Lorestan, Borujerd	LST	33.487N	48.354E	1
Iran	Kordestan, Saghez	SGZ	36.233N	46.267E	2
Iran	West Azarbaijan, Naghadeh	NGD	36.933N	45.367E	2
Syria	Al Raggah	ARG	36.683N	38.950E	2

Appendix 2. (Continued)

Meriones libycus

Country	Locality	Latitude	Longitude	Sample size
Iran	Geno	27.417N	56.183E	1
Iran	Jajarm	36.933N	56.367E	1
Iran	Kashmar	35.183N	57.415E	1
Iran	Sabzevar	29.600N	52.517E	1
Iran	Bajestan	34.517N	58.183E	2
Iran	Kouhak, Zabol	31.067N	61.750E	2
Iran	Garmsar	35.133N	52.183E	3
Iran	Kerman	29.900N	56.533E	3
Iran	Gonbad-e-Kavus	37.233N	55.083E	6
Iran	Shirvan	37.450N	57.917E	4
Iran	Torbat-e-heidariyeh	35.283N	59.217E	4
Iran	Zahedan	29.533N	60.833E	5
Iran	Torbat-e-Jam	35.217N	60.617E	8
Iran	Nehbandan	31.533N	60.033E	8
Iran	Ghoochan	37.100N	58.500E	8
Iran	Sabzevar	36.200N	57.717E	8
Iran	Khash	28.250N	61.200E	9
Iran	Mashhad	36.267N	59.617E	10
Iran	Sarakhs	36.500N	61.050E	9
Iran	Bojnurd	37.467N	57.317E	15
Iran	Dasht, Dashli Borun	37.633N	54.817E	17
Iran	Birjand	32.867N	59.200E	22
Iran	Mansourabad	28.255N	54.034E	23
Iran	Robat e-Gharabil	37.350N	56.317E	3
Iran	Qazvin	36.267N	50.017E	8
Iran	Aghbulagh	35.617N	48.433E	4
Iran	Tehran	35.850N	50.867E	1
Iran	Hamedan	35.700N	48.200E	3
Iraq	Ali al Gharbi	32.464N	46.679E	4
Iran	Ahvaz	31.183N	49.600E	3
Saudi Arabia	Hufuf	25.378N	49.587E	2
Saudi Arabia	Shari wells, NW Arabia and Dwadimi	24.494N	44.383E	8
Syria	Al Qaryatayn	34.233N	37.233E	2
Afghanistan	Kandahar	31.608N	65.705E	2

Appendix 3. Description of the landmarks included in this study

Landmark	Definition
Ventral view	1. Rostral tip of internasal suture
	2. Most lateral junction point of incisive alveolus and body of premaxillary bone
	3. Most rostral point of incisive foramen
	4. Most caudal point of incisive foramen
	5. Most rostral point of palatine foramen
	6. Most caudal point of palatine foramen
	7. Most rostral point on the alveolus of the first molar
	8. Most caudal point on the alveolus of the third molar
	9. Most caudal point of median suture of palatine bone
	10. Most rostral point of foramen magnum
	11. Most lateral point of occipital condyle
	12. Most caudal point of acoustic tympanic bulla
	13. Rostral curvature point at level of the meatus
	14. Most caudal point of zygomatic process concavity formed by temporal bone
	15. Intersection between frontal squama, wing of presphenoid bone and wing of basisphenoid bone
	16. Most lateral point of zygomatic arch at maximum width of skull
	17. Rostral point of zygomatic plate
	18. Maximum curvature of zygomatic plate in infraorbital foramen
	19. Intersection of zygomatic arch and vertical line passing through most caudal point of third molar
	20. Intersection of the zygomatic plate and line connecting the landmarks 13 and 18

Appendix 3. (Continued)

Landmark	Definition
Dorsal view	1. Rostral tip of internasal suture
	2. Intersection of naso-frontal suture with the internasal suture
	3. Intersection of frontal–parietal suture and the interparietal suture,
	4. Intersection of suture between left and right parietals, and parietal–interparietal suture
	5. Midline point of suture between interparietal and occipital
	6. Midline point of caudal margin of the occipital
	7. Most rostral point of suture between nasal and premaxilla
	8. Rostral end of zygomatic plate
	9. Most lateral point of zygomatic plate
	10. Lateral end of the maxillary–frontal suture
	11. Rostral point of upper orbital crest at level of interorbital depression
	12. Intersection of temporal line and suture between parietal and squamosal bones
	13. Tip of concavity of squamosal root of zygomatic arch
	14. Caudal tip of squamosal root of zygomatic arch
	15. Rostrolateral end of tympanic bulla convexity
	16. Caudal end of tympanic bulla on lateral edge of suprameatal process (supramastoid part of squamosal bone)
	17. Distal tip of lateral process of supraoccipital
	18. Caudal end of suture between the mastoid part of tympanic bulla and supraoccipital
	19. Intersection of parietal–interparietal and interparietal–occipital sutures
Lateral view	1. Most rostral point of nasal
	2. Inner extreme point of incisor at body of premaxillary bone
	3. Point at intersection between premaxillary and posterior end of incisive alveolus
	4. Most rostral end of infraorbital foramen edge on zygomatic plate
	5. Most ventral point at the margin of zygomatic plate
	6. Most caudal point of infraorbital foramen on zygomatic plate
	7. Most rostral point of suture between lacrimal and zygomatic plate
	8. Most rostral point of molar on alveolar process of maxilla
	9. Most caudal point of molar on alveolar process of maxilla
	10. Most caudal point of optic canal
	11. Middle of alisphenoid canal
	12. Most caudal point of suture between jugal and squamosal root of zygomatic arch
	13. Intersection between rostral edge of tympanic bulla and most caudal point of gap between tympanic bulla and occipital process of temporal bone
	14. Rostral point of suprameatal triangle
	15. Lateral tip of supraoccipital process
	16. Tip of hamular process of temporal on suprameatal triangle
	17. Rostral end of suture between stylomastoid suture and stylomastoid foramen
	18. Most rostral point of paraoccipital process
	19. Intersection of suture between parietal and supraoccipital with suprameatal process of squamosa
	20. Intersection of temporal line and suture between parietal and squamosal
	21. Junction of suture between parietal and squamosal bone and suture between frontal and squamosal part of temporal bone
	22. Intersection of tympanic part of bulla and line connecting landmarks 16 and 17